

# Control of localized states of itinerant electrons and their magnetic interactions

Yaxin Sun,<sup>1,2</sup> I. S. Lobanov,<sup>3</sup> Jiahao Su,<sup>1,2</sup> Ho-Kin Tang,<sup>1,2,\*</sup> and V. M. Uzdin<sup>3,4,†</sup>

<sup>1</sup>*School of Science, Harbin Institute of Technology, Shenzhen, 518055, China*

<sup>2</sup>*Shenzhen Key Laboratory of Advanced Functional Carbon Materials  
Research and Comprehensive Application, Shenzhen 518055, China.*

<sup>3</sup>*Faculty of Physics, ITMO University, 197101 St. Petersburg, Russia.*

<sup>4</sup>*Faculty of Physics, St. Petersburg State University, 198504. St. Petersburg, Russia*

(Dated: December 2, 2025)

Controlling the magnetic properties of nanosystems by an electric field offers a number of advantages for spintronics applications. Using the noncollinear Alexander-Anderson model, we have shown that the interaction of localized magnetic moments formed by itinerant electrons strongly depends on the position of the d-level relative to the Fermi level, which determines the number of localized electrons. Depending on this parameter, the ground state of the magnetic dimer can be ferromagnetic, antiferromagnetic, or noncollinear without the effects of spin-orbit interaction. The magnetic state can be controlled by shifting the d-level with an electric field, even without current flow. For a sufficiently large value of the hopping parameter between localized states there can be several self-consistent solutions with different values of magnetic moments. This opens new possibilities for manipulation of the magnetic structure of nanosystems. The results obtained lead to a new interpretation of the mechanisms of magnetization reversal, recording, and deleting of magnetic structures in tunneling spectroscopy experiments.

The magnetic properties of 3d transition metals, alloys, and embedded clusters are caused by itinerant electrons. In these systems, the magnetic moments of atoms in Bohr magnetons are not integers and can depend on local configuration, proximity to the surface, interface, or structural defects [1]. Of particular interest is the formation of localized non-collinear magnetic structures, which can serve as bits of magnetic memory [2]. Stability with respect to thermal fluctuations is a key consideration for these applications. However, the calculation of magnetic structures with atomic resolution within the framework of models featuring a continuous magnetization distribution, for example, by density functional theory (DFT), becomes computationally challenging even for systems with just a few magnetic atoms. Consequently, Heisenberg-type models with localized magnetic moments are often employed [3] to analyze the stability and magnetic properties of such small 3d structures [4]. In this context, model parameters are typically chosen to reproduce characteristics obtained from density functional calculations [3–5]. Building on this approach, in the present work we propose a mechanism by which variations in the particle number  $N$  shift a control parameter  $x$ , thereby modulating the interactions between magnetic states and enabling control over the magnetic ordering.

Typically, the parameters of the Heisenberg model can be determined by considering infinitesimal rotations of magnetic moments relative to equilibrium states in certain magnetic configurations. Such configurations can be a collinear ferromagnetic (FM) or antiferromagnetic (AF) state or a non-collinear localized magnetic structure. Generally speaking, the parameters obtained for the

Heisenberg exchange depend on the configuration with respect to which small deviations of the moments are considered [3, 6]. Note that even for a magnetic dimer, for certain values of the parameters in the tight-binding model, the ground state is non-collinear [7]. In the correspondent generalized Heisenberg model, this indicates the need to introduce a biquadratic exchange interaction. A non-collinear structure arises even without taking into account the spin-orbit interaction, which in turn can lead to the appearance of the Dzyaloshinskii-Moriya interaction, which is responsible for formation of non-collinear chiral structures in magnetic systems [3, 8, 9].

Some previous studies claim that an adequate description of the magnetic structure and properties requires going beyond the Heisenberg approximation. This entails accounting for complex interactions such as multispin exchange and configuration-dependent effective interactions, which become significant in noncollinear magnetic regimes [10]. However, the question of the ability of the localized electron model to reproduce all the features of the magnetism of itinerant electrons remains open. What peculiarities of the itinerant model are not accounted for in the generalized Heisenberg model but are important for describing the magnetic behavior and controlling magnetic interactions?

To study this issue, we will consider the simplest system of magnetic dimer within the itinerant non-collinear Alexander-Anderson (AA) model [11]. Initially, the AA model was formulated for the description of two interacting magnetic impurities in the non-magnetic metallic matrix [12]. In the mean-field approximation for Coulomb repulsion on-site, this model is a variant of tight-binding theory. It reproduces many of the results of density functional calculations [13] and to some extent takes into account the effects of electron correlation [14].

The AA Hamiltonian describes the d-impurities in the

\* denghaojian@hit.edu.cn

† valery.uzdin@metalab.ifmo.ru

sea of quasi-free s(p)-electrons of the conduction band. It can be written as

$$H = \sum_{\mathbf{k}, \alpha} \epsilon_k n_{\mathbf{k}\alpha} + \sum_{i, \alpha} \epsilon_i^0 n_{i\alpha} + \sum_{\mathbf{k}, i, \alpha} (v_{i\mathbf{k}} d_{i\alpha}^\dagger c_{\mathbf{k}\alpha} + v_{\mathbf{k}i} c_{\mathbf{k}\alpha}^\dagger d_{i\alpha}) + \sum_{i \neq j, \alpha} v_{ij} d_{i\alpha}^\dagger d_{j\alpha} + \frac{1}{2} \sum_{i, \alpha} U_i n_{i\alpha} n_{i-\alpha} \quad (1)$$

Here  $d_{i\alpha}^\dagger$  ( $d_{i\alpha}$ ) are the creation (annihilation) operators of d-electrons with spin  $\alpha$  ( $\alpha = \pm 1$ ) localized on impurity  $i$  ( $i = 1, 2$ ) with energy  $\epsilon_i^0$  while  $c_{\mathbf{k}\alpha}^\dagger$  ( $c_{\mathbf{k}\alpha}$ ) are the corresponding operators for s(p)-electrons with momentum  $\mathbf{k}$  and energy  $\epsilon_k$  in the conduction band;  $n_{i\alpha} = d_{i\alpha}^\dagger d_{i\alpha}$  and  $n_{\mathbf{k}\alpha} = c_{\mathbf{k}\alpha}^\dagger c_{\mathbf{k}\alpha}$  are the operators of occupation numbers. The parameters of s(p) - d hybridization and direct electron hopping between impurities  $i$  and  $j$  are denoted by  $v_{\mathbf{k}i}$  and  $v_{ij}$ , respectively. The value  $U_i$  defines the Coulomb repulsion of electrons localized on impurity  $i$ .

For the d-subsystem, the presence of the s(p)-conduction band leads to a finite width  $\Gamma$  of d-levels and a shift in their energy, as in the single-impurity Anderson model [15]. The hopping parameter ( $V_{ij}$ ) is also renormalized due to transitions through the conduction band:

$$E_i^0 = \epsilon_i^0 + \text{Re} \sum_{\mathbf{k}} \frac{v_{i\mathbf{k}} v_{\mathbf{k}i}}{\epsilon - \epsilon_k}, \quad \Gamma = \text{Im} \sum_{\mathbf{k}} \frac{v_{i\mathbf{k}} v_{\mathbf{k}i}}{\epsilon - \epsilon_k}, \quad V_{ij} = v_{ij} + \sum_{\mathbf{k}} \frac{v_{i\mathbf{k}} v_{\mathbf{k}j}}{\epsilon - \epsilon_k} \quad (2)$$

To describe the non-collinear structure, we use the mean-field approximation in a local reference frame with the quantization axis along the magnetic moment on each impurity [16, 17]:  $n_{i\alpha} n_{i-\alpha} = \langle n_{i-\alpha} \rangle n_{i\alpha} + \langle n_{i\alpha} \rangle n_{i-\alpha} - \langle n_{i\alpha} \rangle \langle n_{i-\alpha} \rangle$ . After transitioning to a common laboratory frame of reference for both impurity atoms with a quantization axis forming angles  $\theta_i$  and  $\phi_i$  ( $i=1,2$ ) with the directions of the magnetic moment, we obtain the effective Hamiltonian  $H_d^{nc}$  for the d-subsystem.

$$H_d^{nc} = \sum_{j, \alpha} E_j^\alpha n_{j\alpha} + \sum_{j, l, \alpha, \beta} V_{jl}^{\alpha\beta} d_{j\alpha}^\dagger d_{l\beta} - \frac{1}{4} \sum_j U_j (N_j^2 - M_j^2), \quad (3)$$

where

$$\begin{cases} E_j^\alpha = E_j^0 + \frac{U_j}{2} (N_j - \alpha M_j \cos \theta_j) \\ V_{jl}^{\alpha\beta} = \frac{U_j M_j}{2} (\delta^{\alpha\beta} - 1) \delta_{jl} e^{-\alpha i \phi_j} \sin \theta_j + (1 - \delta_{jl}) \delta^{\alpha\beta} V_{jl} \end{cases} \quad (4)$$

Here, the indices  $j$  and  $l$  label the impurity atoms ( $j, l = 1, 2$ ). The Greek indices  $\alpha$  and  $\beta$  correspond to the spin variables. The number of d-electrons  $N_j$  and the magnitude of the magnetic moments  $M_j$  in Eq. (3) and Eq. (4) can be expressed in terms of the Green's function using the following relations [11, 18]:

$$\begin{aligned} N_j &= \frac{1}{\pi} \int_{-\infty}^{\epsilon_F} d\epsilon \text{Im}[G_{jj}^{++}(\epsilon - i\Gamma) + G_{jj}^{--}(\epsilon - i\Gamma)], \\ M_j &= \frac{1}{\pi} \int_{-\infty}^{\epsilon_F} d\epsilon \text{Im}[G_{jj}^{++}(\epsilon - i\Gamma) - G_{jj}^{--}(\epsilon - i\Gamma)] \cos \theta_j + \\ &\quad + \frac{1}{\pi} \int_{-\infty}^{\epsilon_F} d\epsilon \text{Im}[G_{jj}^{+-}(\epsilon - i\Gamma) e^{i\phi_j} + G_{jj}^{-+}(\epsilon - i\Gamma) e^{-i\phi_j}] \sin \theta_j \end{aligned} \quad (5)$$

If we choose the quantization axis in the laboratory system along the magnetic moment of the first atom, then the following expression can be obtained for the Green's functions.

$$G_{11}^{\alpha\alpha} = \frac{1}{\epsilon - E_1^\alpha - \frac{V_{12} V_{21}}{\epsilon - E_2^\alpha - \frac{V_{22}^{\alpha-\alpha} V_{22}^{-\alpha\alpha}}{\epsilon - E_2^{-\alpha} - \frac{V_{12} V_{21}}{\epsilon - E_1^{-\alpha}}}}} \quad (6)$$

The density of states (DOS) with each spin projection is now a superposition of at most four Lorentz contours of width  $\Gamma$ . We will consider a dimer from 2 identical atoms:  $E_1^0 = E_2^0 \equiv E^0$ ,  $U_1 = U_2 \equiv U$ ,  $V_{12} = V_{21} \equiv V$ . The number of d-electrons and magnetic moment on both atoms are also assumed to be the same  $N_1 = N_2 = N$ ,  $M_1 = M_2 = M$ . All energy parameters below will be measured in units of  $\Gamma$ . In the collinear case, the DOS contains only two contours. For parallel moment ordering, their positions are separated by twice the hopping parameter  $V/\Gamma$ , and their amplitudes are the same. The contours for different spin projections are shifted by  $UM/2\Gamma$ . For antiparallel moment ordering, the positions of contours with different spins coincide, but their amplitudes are different.

In the general case equations for the self-consistent determination of the number of d-electrons  $N_1$  and the magnitude of the magnetic moment  $M_1$  can be written as

$$N = \sum_{\alpha} \sum_{\mu=1}^4 \frac{p_{\mu}^{\alpha}}{\pi} \text{arccot} \frac{q_{\mu}^{\alpha} - \epsilon_F}{\Gamma} \quad (7)$$

$$M = \sum_{\alpha} \sum_{\mu=1}^4 \frac{\alpha p_{\mu}^{\alpha}}{\pi} \text{arccot} \frac{q_{\mu}^{\alpha} - \epsilon_F}{\Gamma} \quad (8)$$

In this expression  $q_{\mu}^{\alpha}$  are the roots of the denominator of Green's function Eq. (6), and  $p_{\mu}^{\alpha}$  are the coefficients of its expansion into simple fractions. These quantities depend on  $M$  and  $N$ , as well as on the model parameters  $x = \frac{E^0 - \epsilon_F}{\Gamma}$ ,  $y = \frac{U}{\Gamma}$ ,  $v = \frac{V}{\Gamma}$ . Therefore, (7) and (8) are the equations of self-consistency.

If the magnetic moment  $M$  and the number of particles  $N$  are given, the energy of the system can be found even if  $M$  and  $N$  differ from the equilibrium values. To do this, it is sufficient to integrate the DOS to the Fermi

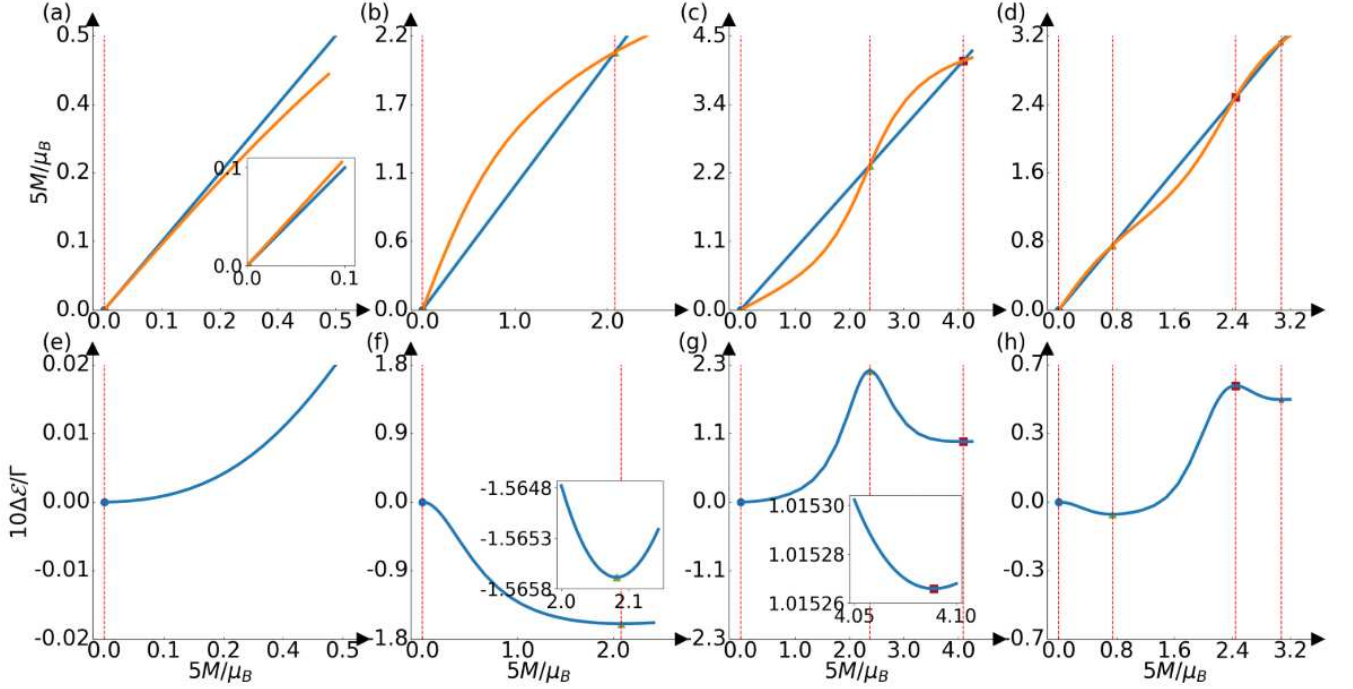


FIG. 1. (Color online) Graphical solution of equation (8) and the dependence of grand canonical potential of dimer  $10\Delta\mathcal{G}/\Gamma$  on  $5M$ . All variants with different numbers of solutions are shown

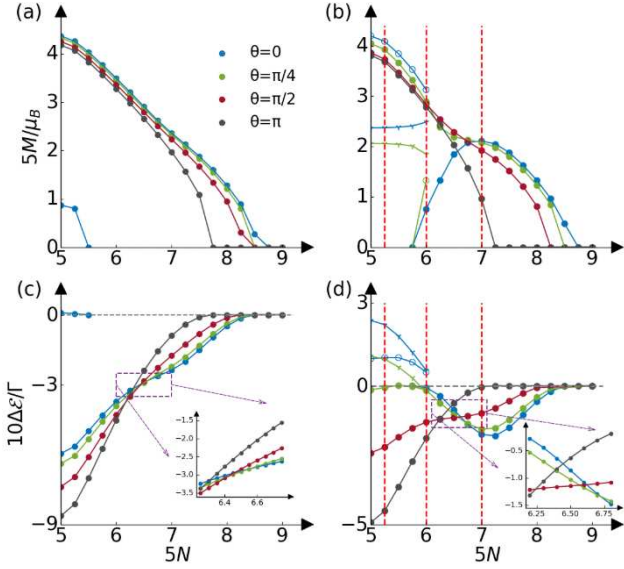


FIG. 2. (Color online) Self-consistent magnetic moment per atom  $5M$  and grand canonical potential of dimer  $10\Delta\mathcal{E}/\Gamma$  as functions of  $d$ -electron numbers  $5N$ . Parameter values:  $y = 13$  (a,c)  $v = 2$ , (b,d)  $v = 3$ . Insets shows the region of non-collinear ground state

the mean field approximation. We define

$$\mathcal{E}(M, N) = \frac{1}{\pi} \sum_{\alpha} \sum_{\mu=1}^4 p_{\mu}^{\alpha} \left[ q_{\mu}^{\alpha} \operatorname{arccot} \frac{q_{\mu}^{\alpha} - \epsilon_F}{\Gamma} + \frac{\Gamma}{2} \ln \left( \frac{(q_{\mu}^{\alpha} - \epsilon_F)^2}{\Gamma^2} + 1 \right) \right] - \frac{U}{4} (N^2 - M^2) \quad (9)$$

where all notations are the same as in right hand Eqs. (7),(8). Then  $\Delta\mathcal{E}(M, N) = \mathcal{E}(M, N) - \mathcal{E}(0, N)$  represents the energy of a state with magnetic moment  $M$ , measured from the nonmagnetic state with the same  $d$ -electron number  $N$ , because contributions from the lower limit of DOS integration in the magnetic and nonmagnetic states will cancel out. Accounting for the fivefold degeneracy of the  $d$ -levels leads to a fivefold increase in the total number of particles  $N$  (7) and the magnetic moment  $M$  (8) on each atom, as well as a tenfold increase in the total dimer energy  $\Delta\mathcal{E}$ .

When the angle  $\theta$  between the magnetic moments changes, the energy surface defined by expression Eq. (9) is also transformed. If we assume that the position of the  $d$ -level relative to the  $\epsilon_F$  defined by the parameter  $x$  remains unchanged, then the number of  $d$ -electrons will adjust and the equilibrium state will correspond to the minimum of the grand canonical potential  $\Delta\Omega = \Delta(\mathcal{E} - \epsilon_F N)$ . In this case, self-consistent solutions will correspond to extrema (minima or maxima) on the  $\Delta\Omega(N, M)$ -surface. Indeed, the conditions  $(\frac{d\Delta\Omega}{dN})_M = 0$  and  $(\frac{d\Delta\Omega}{dM})_N = 0$  coincide with the self-consistency equations Eq. (7) and Eq. (8), respectively.

level and subtract the last term in Eq. (3), obtained in

If the number of particles is fixed,  $N = N^*$ , then changing the angle will adjust the parameter  $x$ , and the equilibrium states with a given angle  $\theta$  correspond to the extrema of the canonical potential. In this case, we can introduce the function  $\Delta(M, x) = \Omega(M, x(N^*, M)) - \Omega(0, N^*, 0)$  where  $x(N^*, M)$  determines the energy  $E^0$  that will give self-consistent values of  $N^*$  (Eq. (7)) for a given magnetic moment  $M$ . If we relate the change in parameter  $x$  to the shift of the Fermi energy with respect to  $E^0$ , we obtain

$$\Delta\mathcal{E}(M, x) = \Delta\Omega(M, x) - \Gamma N^*[x(N^*, M) - x(N^*, 0)]$$

Then condition  $(\frac{d\Delta\mathcal{E}}{dM})_N = 0$  yields the self-consistency condition (8), and  $(\frac{d\Delta\mathcal{E}}{dx})_M = 0$  will provide that the number of d-electrons will be equal to  $N^*$ .

Let us now consider possible solutions of Eq. (8) depending on the number of electrons  $N$ . The corresponding data with dependence on the position of the d-level  $x$  are given in the supplementary materials (SM) [19]. Note that the right-hand side of Eq. (7) is a monotonically decreasing function of  $N$ , while the left-hand side is a monotonically increasing function. Therefore, this equation has a unique solution. Substituting this solution into Eq. (8), we can graphically find possible self-consistent values of  $M$  as shown on the upper panel of Fig. 1. All possible variants of solutions are shown in Fig. 1 together with the dependence of  $\Delta\mathcal{E}(M)$ . The dependencies are plotted for already self-consistent values of  $N$  for the correspondent  $M$ . Note that there is always a nonmagnetic solution. The case when it is the only solution is shown in Fig. 1 (a, e). In this case, adopting the parameters  $N = 8.5$ ,  $\theta_2 = \pi/4$ , and  $v = 2$ , we find that the self-consistent solution occurs at  $M = 0$ , with a corresponding value of  $x = -14.13$ .

In Fig. 1 (b, e) one non-magnetic solution and one magnetic solution are presented. The non-magnetic solution corresponds to the maximum of  $\Delta\mathcal{E}(M, N)$  and is unstable. The magnetic solution represents the ground state. With parameters set to  $N = 7.0$ ,  $\theta_2 = \pi/4$ , and  $v = 3$ , two self-consistent solutions are obtained: one at  $M = 0$  ( $x = -11.95$ ) and another at  $M = 2.10$  ( $x = -11.77$ ).

Fig. 1 (c, f) show the case where 3 self-consistent solutions are possible. The non-magnetic solution is the ground state of dimer. The magnetic solution with a small moment (about  $1 \mu_B$ ) is unstable, and the second magnetic solution with a moment greater than  $4 \mu_B$  are locally stable. For the case of  $N = 5.25$ ,  $\theta_2 = 0$ , and  $v = 3$ , self-consistent solutions appear at the points  $(M, x) = (0, -7.57)$ ,  $(2.35, -6.98)$  and  $(M, x) = (4.05, -7.67)$ .

(d, h) in Fig. 1 show the case where there are four self-consistent solutions of Eq. (8). The non-magnetic solution and the magnetic state with momentum  $2.4 \mu_B$  correspond to the maximum  $\Delta\mathcal{E}(M, N)$  and unstable. The other two magnetic solutions are locally stable. In the ground state the moment is lower. Adopting the parameters  $N = 6.0$ ,  $\theta_2 = 0$ , and  $v = 3$ , we obtain four distinct self-consistent solutions. These can be expressed

as pairs of  $(M, x)$ :  $(0, -9.87)$ ,  $(0.75, -9.52)$ ,  $(2.5, -8.52)$ , and  $(3.15, -8.93)$ .

If we change the  $N$  near a self-consistent solution, leaving the magnetic moment satisfying Eq. (8), it turns out that the minima in Fig. 1 (e, f, g, h) correspond to the minima in  $N$ , and the maxima to the maxima in  $N$ . Thus, the extreme points turn out to be local maxima or minima on the energy surface  $\mathcal{E}(M, N)$ . The same is valid for  $\Omega(M, x)$ , as shown in the SM.

Fig. 2 shows the dependencies of the self-consistent magnetic moment  $5M$  and grand canonical potential of dimer  $10\Delta\Omega$  on the number of d-electrons per atom  $5N$  for different angles  $\theta$ . Figs. 2 (a, c) and (b, d) were obtained for  $v = 2$  and  $v = 3$ , respectively. The dependencies are symmetric with respect to the point  $N=1$ :  $M(2-N) = M(N)$ ,  $\Delta\mathcal{E}(2-N) = \Delta\mathcal{E}(N)$ . The DOS on the first atom for symmetric states satisfies the relation  $\rho_1(\epsilon - \epsilon_F) = \rho_1(\epsilon_F - \epsilon)$ . Only region  $5N > 5$  is presented in Fig. 2.

For both  $v=2$  and  $v=3$ , there is a domain where the ground state is non-collinear. For  $N > 5$  to the left of this region, the ground state is AF with the maximum AF exchange at  $N=5$ . To the right, the ground state is FM. This is consistent with the dependence of the exchange parameter on the Fermi level reported in [6].

For certain values of the parameters in the tight-binding model, a canted ground state of the magnetic dimer was obtained in [7] for closely located magnetic impurities. With increasing distance the interaction became collinear FM or AF. In our case, the noncollinearity behavior does not change qualitatively with variation of the hopping parameter  $v$ , although the strength of the effective interaction and the values of moments decrease with increasing  $v$ .

In the region of noncollinearity of the ground state, the effective exchange stiffness is small, and spontaneous emergence of noncollinear localized magnetic states without DMI and spin-orbit interaction is possible here. Realignment of such structures by a small external action may be of interest for the development of new magnetic memory circuits and other spintronics applications.

Let us now consider the possibility of the existence of several locally stable solutions with different values of the magnetic moments. This qualitatively distinguishes the system under consideration from Heisenberg-type models. For  $v=2$ , several stable solutions are not realized. Only for  $\theta = 0$  does a second self-consistent solution exist, corresponding to the energy maximum, as shown in Fig. 1 e. However non-magnetic state here is unstable with respect to the formation of AF order in the absence of magnetic fields.

At  $v=3$ , multiple solutions exist for  $N$  located between regions with noncollinear ordering. The presence of several solutions occurs with parallel ordering of moments or with small angles  $\theta$  between them. In this case, states with a large angle  $\theta$  or antiparallel ordering are energetically more favorable. Nevertheless, when a magnetic field is turned on that stabilizes states with small  $\theta$ , such

states can be observed, and transitions between them are possible when the field changes. Note that states with an intermediate magnetic moment, which are practically independent of the number of particles, correspond to a local energy maximum. All the possibilities shown in Fig. 1 are realized in Fig. 2 and are marked there with dotted vertical red lines. Based on this finding, we conclude that the particle number has a pronounced effect on the system's interactions, as evidenced by the threefold change in the energy difference.

The possibility of multiple solutions in transition metal nanoclusters on a Cu surface was demonstrated using DFT calculations. However, this was obtained only for clusters larger than a dimer with different electronic states on different atoms [20]. Experiments and calculations on a Co atom on a black phosphorus surface demonstrated the possibility of multiple magnetic states even for a single atom, with different electron configurations of its various orbitals [21, 22]. In all cases, the authors claim the possibility of controlling the different magnetic states using scanning tunneling microscopy (STM). Non-collinear states and multiple magnetic solutions which we found are realized already in 3d-dimer with degenerate d-states.

The dependence of the exchange interaction on the number of particles localized in the dimer atoms allows for a new interpretation of the magnetization reversal mechanisms for magnetic structures observed in STM experiments. They show that to stimulate magnetization reversal, the current  $I$  from the STM tip (and the voltage  $U$  between the tip and the surface) must be sufficiently large [23–26]. The effect is not limited to the release of Joule heat and magnetic field produced by current [23], since at constant power, switching rates depend critically on  $U$  and significantly less on  $I$  [26]. The underlying mechanism is believed to be related to the moments of forces acting on the magnetic structure during current flow. This mechanism explains the different rates of magnetization switching for the current flowing from the tip to the surface and in the opposite direction [23, 26].

The results obtained above suggest another mechanism. As the tip approaches the surface, the associated electric field shifts the d-level and thus changes the electron number  $N$ . For Fe, which carries about seven d-electrons (i.e.,  $5N \approx 7$ ), a reduction in  $N$  lowers the energy of the FM state relative to the nonmagnetic state, but also makes non-collinear configurations more favorable, rendering the system unstable against changes in the moment direction. Conversely, when  $N$  increases, the exchange interaction energy rises relative to the nonmagnetic state, as seen in Fig. 2, making the magnetic structure more susceptible to thermal fluctuations. These effects are not symmetric with respect to the electric-field direction, but in both cases they reduce the lifetime of magnetic states, consistent with experimental observations. Note that the dominant factor is the volt-

age (electric-field strength), while the dependence on the tunneling current is much weaker. Thus, this is another mechanism for controlling magnetic structures using an electrostatic field, which has attracted considerable interest [27, 28]. Electric fields can control magnetic structures by modifying interfacial charge, orbital hybridization, and exchange interactions—allowing reversible tuning of exchange bias and interfacial magnetic order in BiFeO<sub>3</sub>-based heterostructures [29, 30]. Complementarily, spin-transfer torque enables spin-polarized currents to directly switch or reorient magnetic moments, forming the basis of applications such as STT-MRAM and current-driven domain-wall motion [31, 32]. The possibility of manipulating charge topological solitons and bisolitons using an electric field or STM current was recently demonstrated in the experiment [33].

In conclusion, we demonstrated that within the non-collinear AA model for itinerant electrons, the interaction of localized states strongly depends on the occupation numbers of the states. Self-consistent solutions correspond to extreme points on the energy surface, as functions of the d-level position and the magnetic moment. Regions of non-collinear magnetic ordering in a magnetic dimer on a nonmagnetic substrate and regions of the existence of several solutions with different magnetic moments were found. Our work highlights two key findings. First, we demonstrate that the particle number significantly modulates the interaction within the system, manifested as variations between the magnetic and non-magnetic energy states. Second, we uncover a new mechanism for magnetization reversal in nanostructures driven by an external electric field and further influenced by the current from an STM tip.

## ACKNOWLEDGMENT

This work is supported by the National Natural Science Foundation of China (Grant No. 12204130), Shenzhen Key Laboratory of Advanced Functional Carbon Materials Research and Comprehensive Application (Grant No. ZDSYS20220527171407017).

- 
- [1] J. M. Coey, *Magnetism and magnetic materials* (Cambridge university press, 2010).
  - [2] B. Rimmler, B. Pal, and S. S. P. Parkin, *Nat. Rev. Mater.* **10**, 109–127 (2025).
  - [3] A. Szilva, Y. O. Kvashnin, E. A. Stepanov, L. Nordström, O. Eriksson, A. I. Lichtenstein, and M. Katsnelson, *Rev. Mod. Phys.* **95**, 035004 (2023).
  - [4] P. F. Bessarab, G. P. Müller, I. S. Lobanov, F. N. Rybakov, N. S. Kiselev, H. Jónsson, V. M. Uzdin, S. Blügel, L. Bergqvist, and A. Delin, *Scientific Reports* **8**, 3433 (2018).
  - [5] M. Hoffmann and S. Blügel, *Phys. Rev. B* **101**, 024418 (2020).
  - [6] A. I. Lichtenstein, M. I. Katsnelson, and V. A. Gubanov, *J. Phys. F* **14**, L125 (1984).
  - [7] A. Costa, Jr., R. Muniz, and D. Mills, *Phys. Rev. Lett.* **94**, 137203 (2005).
  - [8] M. dos Santos Dias, S. Brinker, A. Lászlóffy, B. Nyári, S. Blügel, L. Szunyogh, and S. Lounis, *Phys. Rev. B* **103**, L140408 (2021).
  - [9] R. Cardias, A. Szilva, A. Bergman, Y. Kvashnin, J. Fransson, S. Streib, A. Delin, M. I. Katsnelson, D. Thonig, A. B. Klautau, and O. Eriksson, *Phys. Rev. B* **105**, 026401 (2022).
  - [10] S. Streib, R. Cardias, M. Pereiro, A. Bergman, E. Sjöqvist, C. Barreateau, A. Delin, O. Eriksson, and D. Thonig, *Phys. Rev. B* **105**, 224408 (2022).
  - [11] P. F. Bessarab, V. M. Uzdin, and H. Jónsson, *Phys. Rev. B* **89**, 214424 (2014).
  - [12] S. Alexander and P. Anderson, *Phys. Rev.* **133**, A1594 (1964).
  - [13] A. Oswald, R. Zeller, P. J. Braspenning, and P. H. Dederichs, *J. Phys. F: Met. Phys.* **15**, 193 (1985).
  - [14] M. I. Katsnelson and A. I. Lichtenstein, *Phys. Rev. B* **61**, 8906 (2000).
  - [15] P. W. Anderson, *Phys. Rev.* **124**, 41 (1961).
  - [16] K. Hirai, *J. Phys. Soc. Jap.* **61**, 2491 (1992).
  - [17] V. M. Uzdin and N. S. Yartseva, *Comp. Mat. Sci.* **10**, 211 (1998).
  - [18] P. F. Bessarab, A. Skorodumov, V. M. Uzdin, and H. Jónsson, *Nanosystems: Physics, Chemistry, Mathematics* **5**, 757 (2014).
  - [19] See Supplemental Material for details.
  - [20] V. Stepanyuk, W. Hergert, P. Rennert, K. Wildberger, R. Zeller, and P. Dederichs, *J. Magn. Magn. Mat.* **165**, 272 (1997).
  - [21] B. Kiraly, A. N. Rudenko, W. M. van Weerdenburg, D. Wegner, M. I. Katsnelson, and A. A. Khajetoorians, *Nat. commun.* **9**, 3904 (2018).
  - [22] D. I. Badrtdinov, A. N. Rudenko, M. I. Katsnelson, and V. V. Mazurenko, *2D Materials* **7**, 045007 (2020).
  - [23] S. Krause, L. Berbil-Bautista, G. Herzog, M. Bode, and R. Wiesendanger, *Science* **317**, 1537 (2007).
  - [24] S. Loth, S. Baumann, C. P. Lutz, D. Eigler, and A. J. Heinrich, *Science* **335**, 196 (2012).
  - [25] A. A. Khajetoorians, B. Baxevanis, C. Hübner, T. Schlenk, S. Krause, T. O. Wehling, S. Lounis, A. Lichtenstein, D. Pfannkuche, J. Wiebe, *et al.*, *Science* **339**, 55 (2013).
  - [26] N. Romming, C. Hanneken, M. Menzel, J. E. Bickel, B. Wolter, K. Von Bergmann, A. Kubetzka, and R. Wiesendanger, *Science* **341**, 636 (2013).
  - [27] N. N. Negulyaev, V. S. Stepanyuk, W. Hergert, and J. Kirschner, *Phys. Rev. Lett.* **106**, 037202 (2011).
  - [28] A. Fert, R. Ramesh, V. Garcia, F. Casanova, and M. Bibes, *Rev. Mod. Phys.* **96**, 015005 (2024).
  - [29] S. Wu, S. A. Cybart, P. Yu, M. Rossell, J. Zhang, R. Ramesh, and R. Dynes, *Nature materials* **9**, 756 (2010).
  - [30] J. Heron, D. Schlom, and R. Ramesh, *Applied Physics Reviews* **1** (2014).
  - [31] J. C. Slonczewski, *Journal of Magnetism and Magnetic Materials* **159**, L1 (1996).
  - [32] L. Berger, *Physical Review B* **54**, 9353 (1996).
  - [33] T. Im, J. W. Park, and H. W. Yeom, *Adv. Mater.*, e10318 (2025).

# Supplemental Material for "Control of localized states of itinerant electrons and their magnetic interactions"

Yaxin Sun,<sup>1,2</sup> I. S. Lobanov,<sup>3</sup> Jiahao Su,<sup>1,2</sup> Ho-Kin Tang,<sup>1,2,\*</sup> and V. M. Uzdin<sup>3,4,†</sup>

<sup>1</sup>*School of Science, Harbin Institute of Technology, Shenzhen, 518055, China*

<sup>2</sup>*Shenzhen Key Laboratory of Advanced Functional Carbon Materials  
Research and Comprehensive Application, Shenzhen 518055, China.*

<sup>3</sup>*Faculty of Physics, ITMO University, 197101 St. Petersburg, Russia.*

<sup>4</sup>*Faculty of Physics, St. Petersburg State University, 198504. St. Petersburg, Russia*

(Dated: December 2, 2025)

The main text presents the dependencies of the magnetic moment  $M$  and the energy  $\Delta\mathcal{E}$  (the canonical potential) of the magnetic dimer relative to its non-magnetic state with the same number of d-electrons. In this case, the self-consistent solutions corresponded to the extrema of  $\Delta\mathcal{E}$ , considered as a function of the magnetic moment  $M$  and the parameter  $x$ , which determines the position of the d-level relative to the Fermi level.

The dependencies of the magnetic moment  $M$  and the grand canonical potential  $\Delta\Omega$  on  $x$  are given here. The self-consistent solutions correspond to the extrema of  $\Delta\Omega(M, N)$  with respect to  $M$  and  $N$ . Fig. ?? shows the dependencies of  $M(x)$  and  $\Delta\Omega(x)$  for  $v = 2$  and  $y = 13$ . The colors display different angles  $\theta$  between the magnetic moments in the dimer.

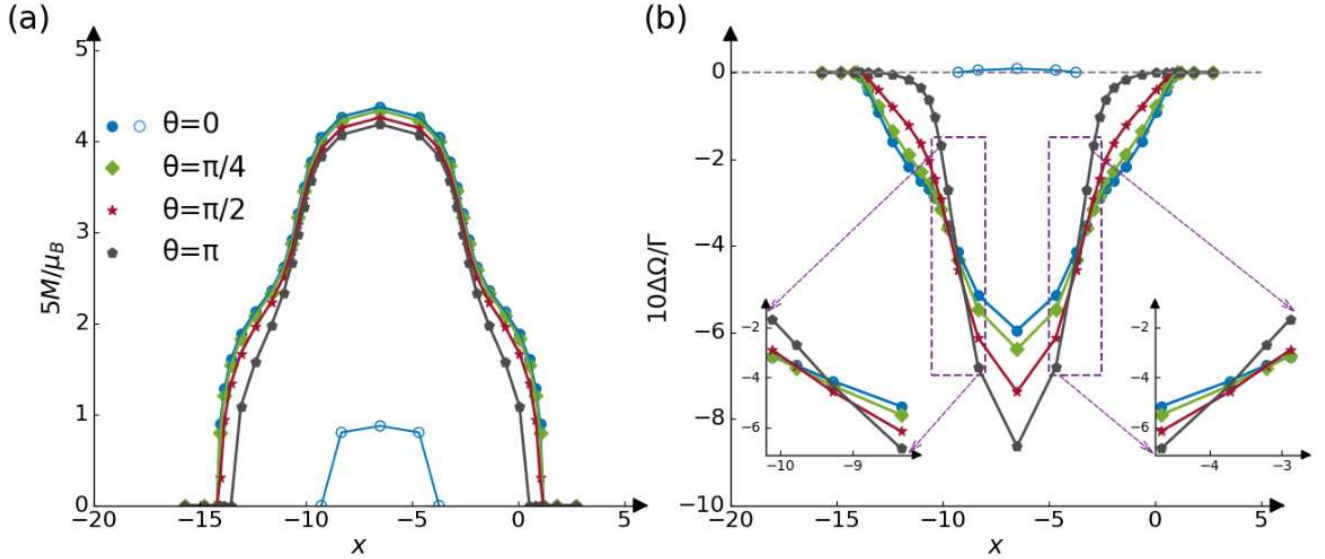


FIG. S1. (Color Online) The magnetic moment of each atom and the grand canonical potential of the magnetic dimer as a function of  $x$ . Values of parameters are  $v = 2, y = 13$ . Individual colors indicate the angles between the magnetic moments. Filled and empty symbols correspond to the ground and unstable states, respectively. The inset shows the non-collinear ground state regions at a larger scale.

As can be seen, the magnitude of the moments depends weakly on the angle  $\theta$ . All dependencies are symmetric about the point  $x = -6.5$ , which corresponds to the half-filled band. There are regions of non-collinear ordering between the states corresponding to ferromagnetic and antiferromagnetic states; these regions are shown in the insets on a larger scale.

Fig. ?? shows the evolution of the  $x$ -dependence of the magnetic moment of the dimer atoms and the grand canonical potential of the dimer with a change in the angle  $\theta$  between the magnetic moments. At small  $\theta$  there are several self-consistent solutions for the same value of  $x$ . Magnetic solutions can correspond to the ground, metastable, and unstable states. The first two correspond to local minima of  $\Delta\Omega$ , as a functional of  $M$  and  $x$ . They are shown in

\* [denghaojian@hit.edu.cn](mailto:denghaojian@hit.edu.cn)

† [valery.uzdin@metalab.ifmo.ru](mailto:valery.uzdin@metalab.ifmo.ru)

the figure in blue and green. In the latter case, a local maximum is observed, and the corresponding curve is colored orange.

For  $\theta > \pi/2$ , only one magnetic solution is possible. Near the half-filled band, the ground state corresponds to an antiferromagnetic ordering of the moments. However, as can be seen in the fig. ??(f), there is a region with red squares where the ground state is non-collinear.

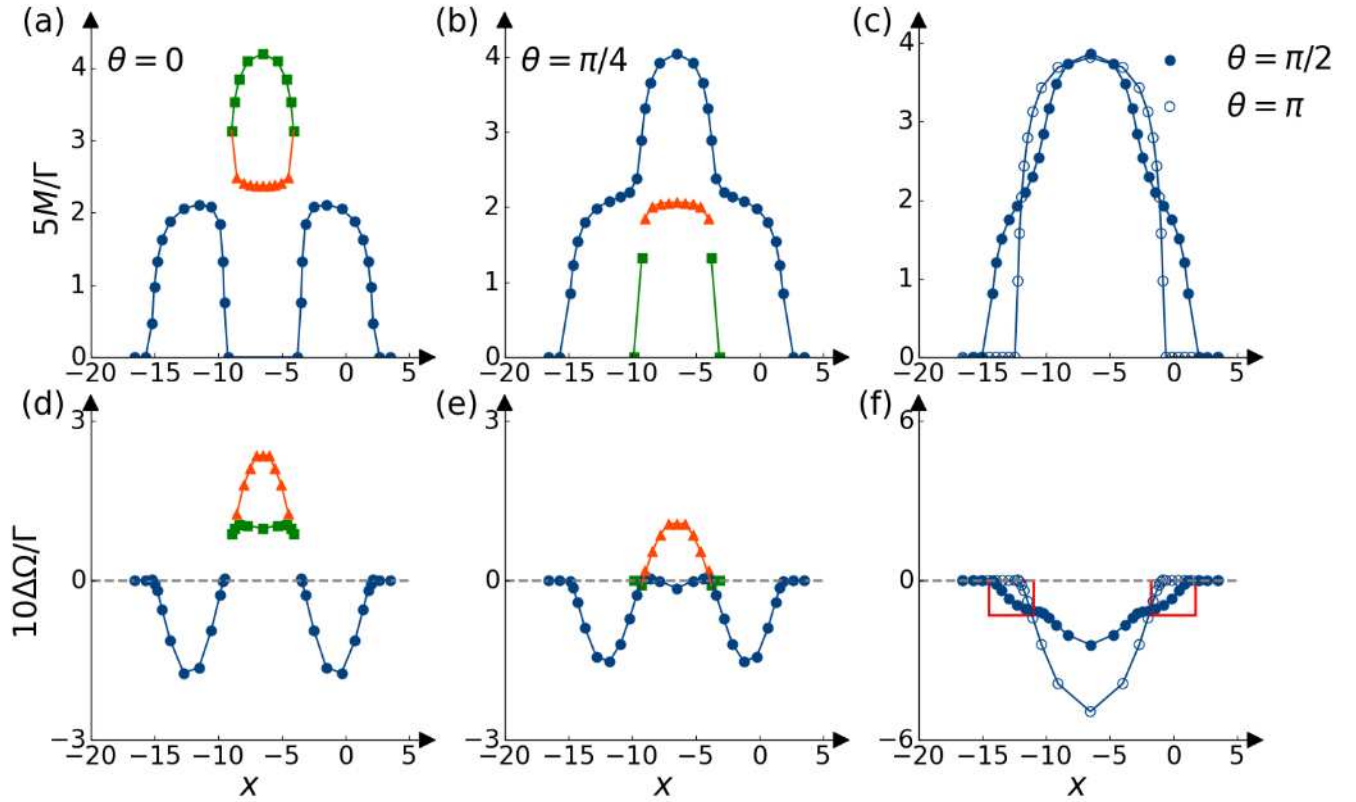


FIG. S2. (Color online) Dependence of the magnetic moment per atom and the grand canonical potential of a magnetic dimer on the parameter  $x$  for different angles  $\theta$ : (a),(d) –  $\theta = 0$ ; (b),(e) –  $\theta = \pi/4$ , (c),(f) –  $\theta = \pi/2$  and  $\theta = \pi$ . Parameter values:  $v = 3, y = 13$ .